WATER MIST SUPPRESSION OF METHANE/AIR AND PROPANE/AIR COUNTERFLOW FLAMES

E.J.P. Zegers, B.A. Williams, R.S. Sheinson, and J.W. Fleming
Naval Research Laboratory

INTRODUCTION

Water possesses many attributes of the ideal fire suppressant. It is nontoxic. noncorrosive, ubiquitous. and has no adverse environmental effects. Water aerosols offer substantial cooling capacity, due both to water's relatively high heat capacity per unit mass, and also the enthalpy of vaporization obtained when water is added in the liquid phase. Conventional sprinkler systems typically produce sprays of droplets with diameters on the order of a millimeter [I]. These systems typically require a far greater thermal mass of agent to suppress a given fire than that needed for gaseous agents. Application of water in the form of mist (which generally refers to droplets smaller than 200 μm) offers several advantages. Because smaller droplets have larger surface to volume ratios and longer suspension times in quiescent air, vaporization in the vicinity of the fire is greatly improved. Less water is therefore required to accomplish extinguishment, and liquid water residue is minimized. Small droplets also follow the flowfield of the combustion gases more closely, and thus have the capability of reaching obstructed areas.

Nevertheless, a number of issues arise that impact the practical implementation of water mist systems in many applications. Producing very small droplets in sufficient number densities to accomplish extinction generally requires more sophisticated generation and delivery systems than would be needed for larger droplet sizes. Also, the coverage obtainable from a single nozzle. the droplet suspension time, and the ability to suppress obstructed fires, are all critical to the effectiveness of a water-based tire suppression system [I]. Many of these factors do not come into play for gaseous agents. For these reasons, optimal use of water mist systems requires detailed knowledge of the behavior and suppression effectiveness of water in the vicinity of a flame as a function of droplet size as well as the gas flow field.

A comprehensive review has recently been published summarizing studies of the use of water against Class A (combustible solid) fires [I]. In contrast. many of the most serious fire threats faced in military applications are Class B (flammable liquid). Nevertheless, many aspects of droplet characteristics, system design, and modes of suppression are common to both fire types.

The details of the interaction between water mists and flames have not yet been fully characterized. Water is generally thought to suppress combustion primarily through physical mechanisms [2, 3], chiefly through reduction of the adiabatic flame temperature, as well as dilution of the reactants. The behavior of the droplets in the combustion flow field dictates where the droplets evaporate, whether they evaporate completely or not, the impact they have on the reaction zone, and thus the effectiveness of the mist. Critical to all these issues is the size distribution of the droplets. Lenrati and Chelliah [3, 4] conducted modeling studies of the behavior of water mists in methane/air counterflow flames. They predicted that the best suppression effectiveness should he obtained at droplet sizes between 20 and 30 μm. Droplet sizes below 20 μm were predicted to be slightly less effective, although the suppression effectiveness was predicted to be relatively insensitive to droplet size up to 30 μm. Above this size effectiveness was predicted to diminish steadily with increasing droplet size. Experimentally, suppression of counterflow flames by water has been investigated by Seshadri [5], using very small droplets that vaporized completely.

Here, we investigate initially monodisperse water mists (meaning that all droplets are of nearly equal size) having droplet sizes between 14 and 44 μm, in non-premixed counterflow propane/air flames. We measure droplet velocities, evolution of droplet size distribution in the vicinity of the flame zone, and droplet suppression effectiveness, as a function of droplet size.

Knowledge of the behavior of droplets, as a function of size, for various flame conditions is an important consideration in system engineering. Smaller droplets evaporate more easily, giving better cooling and more oxygen dilution for a given amount of water. On the other hand, producing smaller droplets in sufficient quantity generally requires higher water pressures at the nozzle, a significant engineering drawback. **Also,** the "throw distance," which dictates the area coverage achievable by a single nozzle. is reduced for small droplets, which carry less momentum and are more susceptible to aerodynamic drag.

EXPERIMENTAL SETUP

The counterflow burner used to conduct the water mist experiments has been described previously [6,7]. Figure 1a shows a diagram of the burner setup. Propane flows from the top tube. The mist is supplied in the air stream from the bottom tube. The tubes are housed in a Plexiglas chamber that is continuously purged with nitrogen. Both tubes have inner diameters of 10 mm and are 10 mm apart. The tubes are approximately 80 cm long, allowing a parabolic velocity profile to develop fully. Flow straighteners were not used. The gas velocity profiles near the tube exits are flattened slightly, due to the presence of the opposing flows. In the configuration used for the present experiments, the luminous flame zone is fairly flat.

For gaseous reactants in this configuration, we have previously measured a relationship between the local strain rate (by which we refer to the maximum gradient of axial velocity on the air side of the reaction zone), the burner gap size, reactant velocities, and densities [7]. This burner specific relationship is used in the present study to calculate local strain rates, and has been previously shown to remain valid for the addition of gaseous agents of high molecular weight to the air stream. For a condensed phase agent, the situation becomes more complicated, because under some conditions the condensed phase may comprise a substantial fraction of the total momentum of the flow, but not have the same velocity as the surrounding gas. In determining strain rates in the present study, we have assumed that the gas flow field is unchanged by the presence of the water mist. This approximation is only valid if the mass fraction of water in the air stream is small. For larger water mass fractions, the gas flow field must be measured in the presence of the water droplets. The velocities of the water droplets themselves cannot be used to determine the gas flow velocity, however, because they are too large to follow the gas flow field. For these reasons, we restrict the present study to water mass fractions in the air stream of $< 3\%$.

The mists are produced using a vibrating orifice aerosol generator (TSI Inc. Model 3450), based on the design of Berglund and Liu [8]. A schematic of the droplet generator is shown in Figure 1b. Water is forced through a pinhole that is acoustically excited by a piezoelectric ceramic. At specific resonant frequencies, the water jet breaks up into a monodisperse droplet stream. This stream exits the generator through a hole in the dispersion cap. By forcing air to exit through this same hole, the droplet stream is dispersed into a cloud as it exits the droplet generator and enters the counterflow burner's bottom tube. Measurements of droplet number density as a function of radial position at the tube exit indicated that the droplets are evenly distributed except near the tube wall. The mass flow rate of water is adjusted primarily by controlling the backing pressure of water entering the orifice. The use of the small orifice in this type of droplet

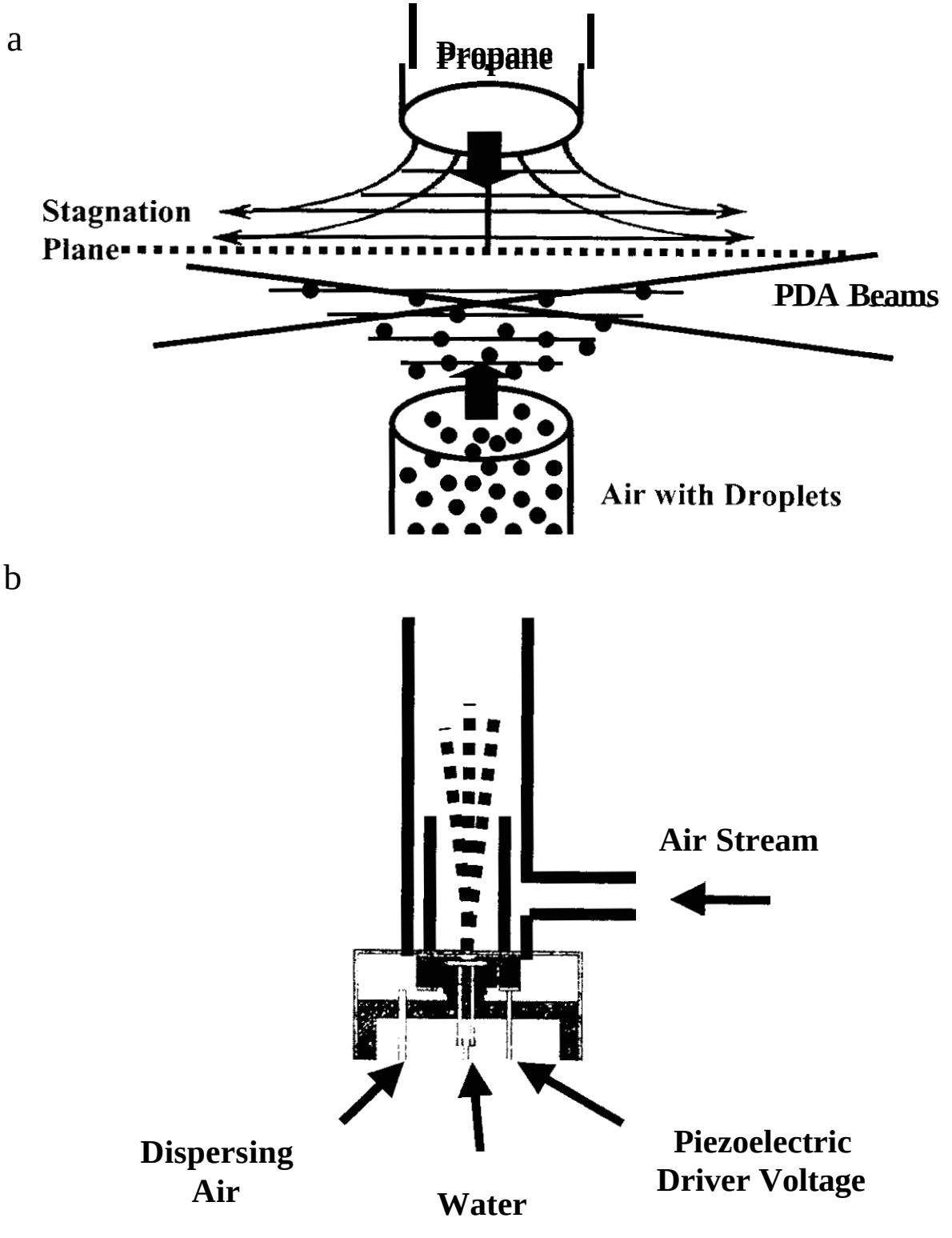

Figure 1. (a) Counterflow burner for water mist studies: (b) Piezoelectric droplet generator.

generator places limitations on the achievable water flow rate. In general, the smaller the orifice used, the smaller the maximum flow rate of water that could be obtained.

To obtain flame conditions of high strain rate and low water mass fraction, the aerosol was mixed with a secondary (dry) air stream. The mixture was then introduced up the lower tube toward the reaction zone. For low strain rate conditions, the air flow rate through the droplet generator required to accomplish droplet dispersal often exceeded desired total air flow rate to the burner. Under these conditions, a portion of the air/droplet stream was diverted to bypass the burner. The flow rate of air diverted was measured after trapping the entrained droplets. In the analysis below, we assume that no collisions between droplets occur. The volume fraction occupied by droplets for our conditions is typically $1\text{-}2 \times 10^{-5}$. The assumption that a significant number of collisions do not occur is consistent with the droplet size histograms, which do not show appreciable droplet growth, as would be the case if collisions leading to coalescence of drops were to occur.

The aerosol generator used in the present study produces droplets having very narrow size distributions. When the dispersion air is used, 95% of the droplets have diameters within a $<5\mu m$ range, the size distribution is even narrower in the absence of dispersion air. One limitation of this generator is that the droplet diameter cannot be continuously adjusted. Monodisperse droplets can only be produced at specific sizes, corresponding to piezoelectric driver frequencies that match acoustic resonances of the orifice. Using a 5 μm diameter pinhole, for example, monodisperse droplet streams with a size distribution peak at diameters of 14, 18, and 24 μm have been produced. With a $10\mu m$ diameter pinhole, monodisperse streams of 25, 30, and 37 μm droplets have been obtained. If the piezoelectric driver frequency is nonresonant, a bimodal or multimodal droplet size distribution generally results.

Droplet size and velocity distributions were monitored using a Phase Doppler Particle Anemometer (PDPA-Dantec Measurement Technology). Based on this technique, droplet diameters, axial velocities, and number densities are measured at discrete points in the flame by recording each droplet that crosses the probe volume formed by the intersection of the two probe laser beams during a specified time period. Laser light scattered by the droplets was collected through a window mounted in the Plexiglas chamber. The burner is mounted on a three-axis translation stage, such that the laser probe volume could be positioned anywhere in the gap between the opposed tubes, to record droplet characteristics as a function of position. In the present investigation, the axial position of the flame is determined by centering the PDPA probe volume in the middle of the flame's visible emission zone.

The droplet size distribution was monitored during experiments, to ensure that the piezoelectric driving frequency was correctly chosen to yield a monodisperse droplet distribution. The droplet volume density determined by the PDPA was the primary determination of the amount of liquid water delivered to the flame. Comparison runs between the PDPA determination of the water delivery rate, and direct measurements of the accumulated mass of water exiting the droplet generator, yielded agreement within a few percent. The PDPA system was capable of acquiring data at higher droplet loadings than those reported here. This was verified in the case of the larger droplet sizes (the achievable mass fraction of the smaller droplets was limited by the generator). The limit on the water mass fraction in the data presented here is due to the effect of the water droplets on the strain rate, not a limitation of the PDPA diagnostic.

RESULTS

DROPLET BEHAVIOR

Figures 2a and 2b show the evolution of the droplet size distribution, in propane/air counterflow flames, of initially monodisperse water mists of 30 and 18 μm, respectively. The figures plot number densities of droplets in various size ranges as a function of axial position (x), along the burner's axis (r = 0 mm). The local axial strain rate (K) imposed on the flames corresponds to approximately 30% of the extinction strain rate measured in the present apparatus [7] for the uninhibited flame ($K_{ext} = 608 \pm 65\ s^{-1}$). The air and droplets exit the lower tube at x = 0 mm: the propane exits the upper tube at x = 10 mm. The luminous zones of the flames are located at x = *5.0* and 4.5 mm. respectively, in the experiments employing 30 and 18 μm mists. For both initial sizes, the diameter of the droplets changes very little until the flame is reached, with the 30 or 18 μm droplets dominating the size distribution.

In the flame region. the two droplet sizes show somewhat different behaviors. In both cases, the droplets evaporate, and the total number density of droplets summed over all size ranges decreases. For the 18 μm initial droplet size, virtually no droplets of any size are detected once the flame is reached. For the 30 μm initial size, the total number density decreases, though not as dramatically, in passing through the flame zone. The droplets that are detected in or beyond the flame zone have a broad size distribution, and a much smaller average size than do the incident droplets. These observations indicate that, for this flame condition, the 18 μm droplets undergo essentially complete vaporization once they enter the reaction zone, while the 30 μm droplets appear to be near the threshold size above which droplets are not completely evaporated. When incident droplets of 44 μm diameter were used, a much larger number of droplets was detected beyond the flame zone, supporting the assertion that 30 pin is close to the minimum size capable of surviving penetration into the flame.

Figures 3a and 3b focus specifically on the number density profiles of the 30 and 18 μm droplets respectively. Number density is plotted versus axial position. In both experiments. the density first increases with axial position, then quickly drops in the flame region. Three effects combine to explain the shape of the number density profiles. (1) The main effect is related to the velocity profiles of the 30 and 18 μm droplets, provided in Figures 3a and 3b respectively. At the lower tube exit. the droplets have roughly the same velocity as the gas stream. **As** the gas stream's axial velocity changes in the counterflow field, the equilibrium in velocity between the liquid and gas phases is lost. and the drag forces act to reestablish it. The droplet velocity profile therefore follows that of the gases: the velocity initially drops as the gases move towards the stagnation plane; it then increases when the hot gases expand in the reaction zone, before it drops down again, close to the stagnation plane. In regions where the droplets are decelerating. faster droplets catch up to slower ones, and the number density will tend to rise. In the flame region, the droplets accelerate, which tends to reduce their number density. Figures 3a and 3b show that the impact of axial velocity gradients on droplet number density is significant. with variations in number density well correlated with variations in velocity. *(2)* As the air exits the lower tube, the flow streamlines begin to diverge in the counterflow field, producing radial drag forces on the mist. Due to this effect, the droplets move away from the burner axis. The divergence of the air flow therefore acts to reduce the droplet number density along the centerline. (3) Evaporation in the flame region causes the droplet size to decrease, and thus also contributes to the decrease in the number densities of the 30 and 18 pm droplets.

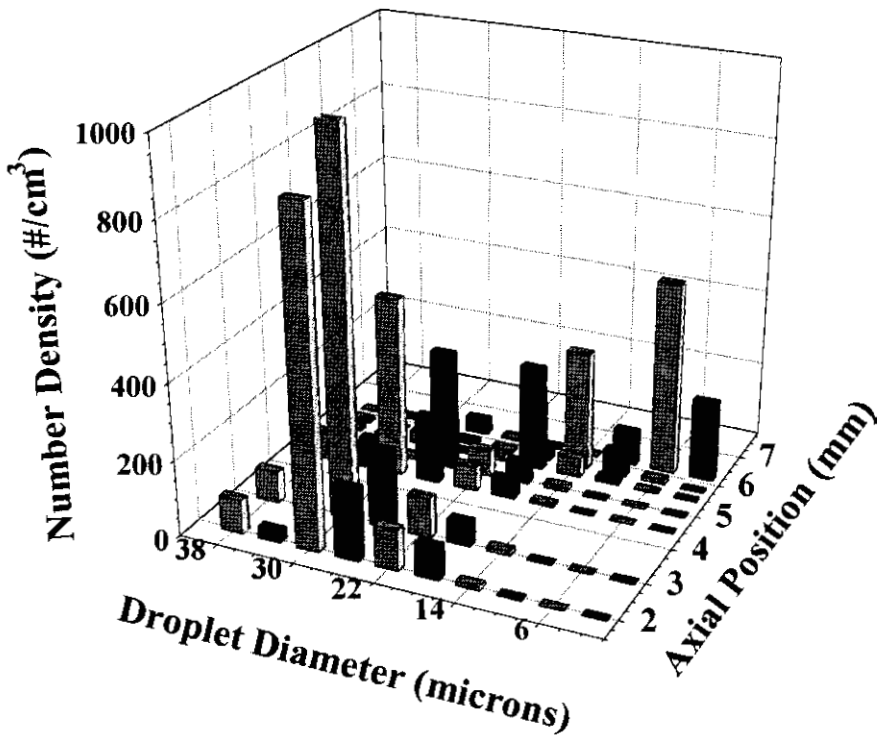

Figure 2a. Droplet **size** distribution evolution for a 30-pm water mist in a $170 s^{-1}$ strain rate flame. The luminous flame is centered at 5 mm.

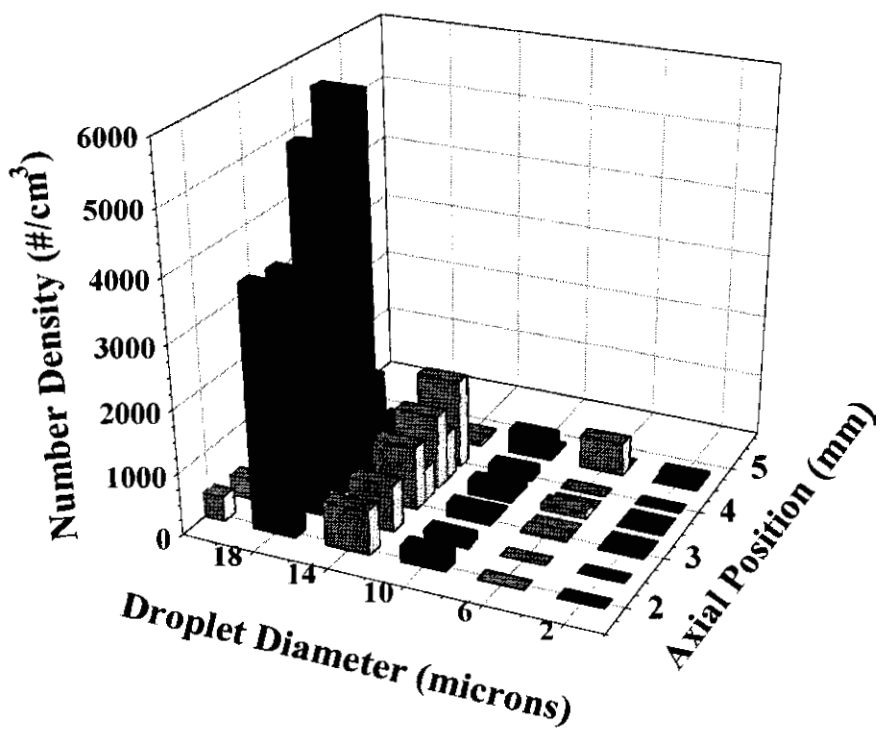

Figure ›. Droplet size distribution evolution of an 18-μm water mist in a $170 s^{-1}$ strain rate propane/air counterflow flame. The luminous flame is centered at 4.5 mm.

When the data of Figure 3 are plotted in terms of droplet tlux rather than number density, the peak just before the reaction zone is not present. Figure 4 shows the droplet flux profile for the 30 μm mist. The flux was determined from the PDPA software by summing over all droplets detected within the measurement time, with the sum weighted by the velocity of each drop. The droplet flux decreases slightly as the flame is approached, under the effects of the diverging flow and evaporation. The flux then decreases dramatically in passing through the high temperature zone. For the 18 μm incident droplet size, the plot of flux versus position is qualitatively similar to that of the 30 μm droplets, except that the flux drops to essentially zero once the reaction zone is reached. In the plots of droplet flux, scatter in the data is attributable in part to experimental uncertainties, in the PDPA concentration measurements in particular. Slight variations in the position of the flame over the course **of** the experiment also contribute to the scatter.

FLAME EXTINCTION

We have measured the extinction strain rates of non-premixed propane/air counterflow flames at various water mass fractions (up to 3%) at droplet sizes of 14, 30. and 44 μm. Droplet fluxes were measured by the PDPA instrument along the burner axis 2.0 mm from the air tube exit. at strain rates within 10% of extinction. Local strain rates were determined from the gas tlows as discussed above. The results are plotted in Figure 5. For comparison, extinction mass fractions of Halon I301 versus local strain rate in the propane/air counterflow flame [7] are also plotted. The 44 μm water droplets are clearly much less effective in reducing the extinction strain rate than are the 14 or 30 μm droplets. The 14 pin droplets appear to be slightly more effective than the 30 μm, but a direct comparison is difficult, because only a very limited mass fraction of water was obtainable in the 14 μm droplet size with the present generator. Both of the smaller droplet sizes are more effective in reducing the extinction strain rate than is Halon 1301.

DISCUSSION

Li, Libby, and Williams [9] performed both numerical and analytical modeling, as well as experimental measurements, of the behavior of methanol droplets in opposed flows, both in the presence and absence of a flame. Clearly. there are differences between the interaction of a fuel droplet with a flame, and that of a suppressant droplet. Nevertheless. the effects of evaporation and of viscous drag imparted by the local gas flow field should have analogies between the two cases. Li et al. [9] documented and analyzed the phenomenon of "pushback" previously described by Chen et al. [10], in which droplets in certain size ranges exhibit oscillatory motion in the vicinity of the stagnation plane. For a given flow field. large droplets tend to oscillate, while small droplets asymptotically approach an equilibrium position slightly below the stagnation plane. Under the assumptions of the Stokes drag law, neglect of evaporation, and an axial strain

$$R_{\min} = \left(\frac{9\mu}{8\rho K} \right)^{1/2} \qquad (1)$$

rate independent of axial position, the minimum droplet radius for oscillation to occur is given by where μ is the absolute viscosity of the surrounding gas, ρ is the droplet density, and K is the axial strain rate. For a water droplet in air at a strain rate of 150 s^{-1}, the minimum diameter for oscillation to occur is approximately 30 pm. In practice, this threshold represents a lower bound because all droplets lose mass by evaporation, and water droplets with initial sizes smaller than the oscillation threshold usually undergo complete vaporization upon entering the flame zone [4]. The size ranges of droplets investigated in the present study bracket the threshold size for oscillation for the present flowfield conditions. Furthermore, the threshold sire is similar to the

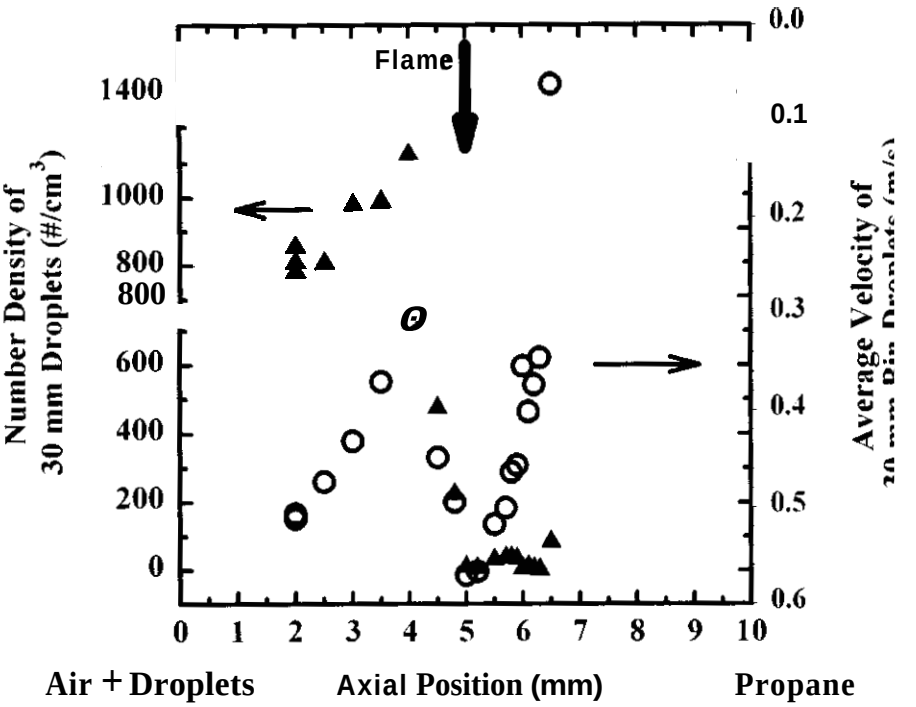

Figure 3a. Profiles of number density (triangles) and velocity (circles) for 30-pm water droplets versus location in a 170 s^{-1} strain rate propane/air/30-μm mist counterflow flame.

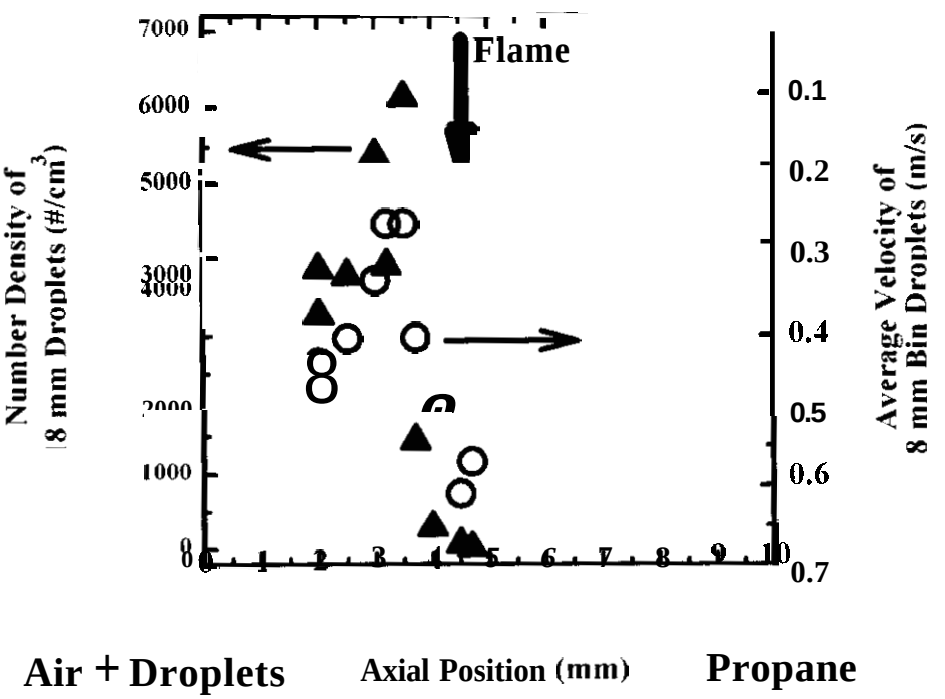

Figure **3b.** Profiles of number density (triangles) and velocity (circles) of 18-μm water droplets versus location in a propane/air/18-μm mist counterflow flame.

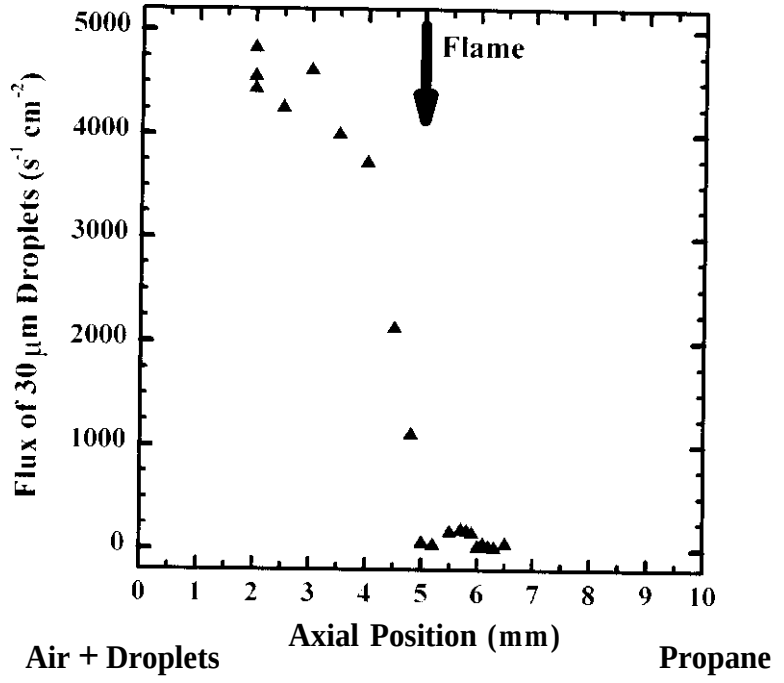

Figure 4. 30-ym droplet **flux** profile for a 30-μm water mist in it I70 s^{-1} strain rate propane/air flame.

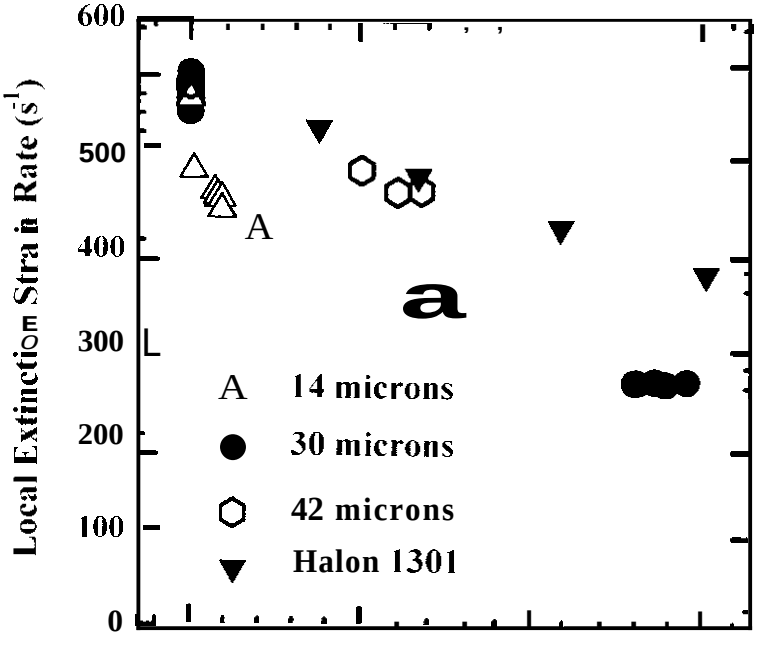

Figure 5. Extinction strain rate for propane/air flames versur **mass** fraction of added water mirt or Halon 1301 in **the** air stream.

size predicted by Lentati and Chelliah to be most effective at suppression, although this could be a consequence of the relative importance of viscous drag and evaporation for water in particular. The present experimental results are consistent with the numerical predictions of Lentati and Chelliah for monodisperse droplet streams in a number of respects. For a methane/air counterflow flame with a local strain rate of 130 s-', it was predicted [4] that a 30 μm water droplet should just pass through the reaction zone before evaporating completely. In contrast, droplets having diameters I5 μm or less should completely evaporate before reaching the location of maximum temperature. The data shown in Figs. 2 and 3 are taken with a different fuel (propane vs. methane) and at a slightly higher strain rate (165-175 s^{-1} versus 130), but show the same qualitative behavior as a function of droplet size. Furthermore, Lentati and Chelliah [3] predicted that appropriately sized water droplets could be more effective on a mass basis than Halon 1301 in suppressing combustion. This conclusion is in accord with a prediction of water's suppression efficiency [11] based on an empirical model comparing its properties with those of other inert agents, according to which water should be *50%* more effective than CF_3Br. Lentati and Chelliah [3] predicted that the effectiveness of water was likely to decrease significantly with increasing droplet size for diameters >30 μm. Both of these predictions are consistent with the data presented in Figure 5. There were approximations made in modeling [3, 4], as well as nonideality in the present experiment. Nevertheless, our findings indicate that the predictions of Lentati and Chelliah are largely correct, at least in those aspects for which the present data provides an adequate validation test.

CONCLUSIONS

Using piezoelectric generation of aerosol droplets, we have investigated the evolution of velocity and size distributions of initially monodisperse, 30 μm and 18 μm water mists in non-premixed propane/air counterflow flames. For both size mists, the peak in the droplet size distribution does not change until the flame zone is reached. The peak then shifts to smaller diameters due to evaporation. Variations in number density with axial position are strongly correlated with variations in droplet axial velocity. The fluxes of both 30 and 18 μm droplets decrease between the air tube exit and the stagnation plane, due to the effects of the diverging flow and evaporation. For both 30 and 18 μm mists, very few droplets survive the flame, suggesting that, for these size droplets, in a counterflow flame at moderate strain rate, most of the suppression potential of the mist is being used.

On a mass basis, both 14 μm and 30 μm diameter mists were found to be more effective than Halon 1301 at suppressing non-premixed propane/air counterflow flames. The flame inhibition properties of the 44 μm diameter mist were considerably poorer than those of the 14 or 30 μm mists. The lower suppression efficiency of the 44 μm mist parallels previous predictions of numerical modeling, and appears to be caused by incomplete droplet vaporization during passage through the reaction zone. The present findings indicate that, if the delivery issues inherent to a condensed phase fire suppressant can be successfully addressed, water is capable of achieving suppression effectiveness comparable to that of CF_3Br.

In terms of practical issues, it is worth noting that many spray or mist generators used in fire-fighting produce droplet distributions which are quite broad. The quoted size of the droplets is typically some "mean" droplet size. Several different definitions of a mean are commonly used: diameter, surface area, volume, ratio of volume to surface area, etc. For a non-monodisperse droplet distribution, a single number can only provide a limited amount of information about a distribution; two droplet generators may produce droplet distributions with the same mean size,

but very different populations of droplets in various size ranges. Optimization of the performance of a non-monodisperse droplet distribution is an issue for future work.

ACKNOWLEDGMENTS

This research is sponsored by the US Department of Defenses Next-Generation Fire Suppression Technology Program funded by the DoD Strategic Environmental Research and Development Program.

REFERENCES

1. Grant, G., Brenton. J., and Drysdale, D., "Fire Suppression by Water Sprays," *Prog. Energy Combust. Sci.* 26, p. 79, 2000.

2. Dlugogorski, B.Z., Hichens, R.K., Kennedy, E.M., and Bozzelli, J.W.. "Propagation of Laminar Flames in Wet Premixed Natural Gas-Air Mixtures," *Trans. **Inst.** Chem. Eng.* B 76, p. 81, 1998.

3. Lentati, A.M., and Chelliah, H.K.. "Physical, Thermal, and Chemical Effects of Fine Water Droplets in Extinguishing Counterflow Diffusion Flames," *Twenty-Seventh Symposium (International) on Combustion,* The Combustion Institute, Pittsburgh. pp. 2839-2846, 1998.

4. Lentati, A.M., and Chelliah. H.K., "Dynamics of Water Droplets in a Counterflow Field and Their Effect on Flame Extinction," *Combustion and Flume* 115, p. 158, 1998.

5. Seshadri. K., "Structure and Extinction of Laminar Diffusion Flames Above Condensed Fuels with Water and Nitrogen," *Combustion and Flume* 33, p. 197, 1978.

6. Papas. P.. Fleming. J.W., and Sheinson, **R.S.,** "Extinction of Non-Premixed Methane- and Propane-Air Counterflow Flames Inhibited with CF_4, CF_3H, and CF_3Br," *Twenty-Sixth Symposium (International) on Combustion,* The Combustion Institute, Pittsburgh. p. 1405, 1996.

7. Zegers, E.J.P., Williams, B.A., Fisher, E.M., Fleming, J.W., and Sheinson, R.S., "Suppression of Nonpremixed Flames by Fluorinated Ethanes and Propanes," *Cornbustion and Flume* 121, p. 471, 2000.

8. Berglund, R.N.. and Liu. B.Y.H., "Generation of Monodisperse Aerosol Standards." *Environ. Sci. Technol.* 7, p. 147, 1973.

9. Li, S.C., Libby, P.A., and Williams, F.A.. "Spray Structure in Counterflowing Streams With and Without a Flame,'' *Combustion and Flame* 94, p. 161, 1993.

10. Chen, N.-H., Rogg, B., and Bray, K.N.C., "Modeling Laminar Two-Phase Counterflow Flames with Detailed Chemistry and Transport," *Twenty-Fourth Symposium (International) on Combustion,* The Combustion Institute, Pittsburgh, p. 1513, 1992.

11. Sheinson. R.S.. "Laboratory Through Full Scale: The U. S. Navy Halon Total Flooding Replacement Program," in *Halon Replacements: Technology and Science*, **ACS** Symposium Series 611, Miziolek. A. W., and Tsang, W. (eds.), American Chemical Society, Washington. DC, pp. 175-188, 1995.